Real-time experimental data of the muon hodoscope URAGAN accessible in www

2015 J. Phys.: Conf. Ser. 632 012086

(http://iopscience.iop.org/1742-6596/632/1/012086)

Real-time experimental data of the muon hodoscope URAGAN accessible in www

I I Yashin, I I Astapov, N S Barbashina, V V Borog, A N Dmitrieva, D V Chernov, R P Kokoulin, K G Kompaniets, Yu N Mishutina, A A Petrukhin, V V Shutenko, O A Sit'ko, E I Yakovleva

National Research Nuclear University MEPhI
(Moscow Engineering Physics Institute), 115409, Moscow, Russia

E-mail: iiyashin@mephi.ru

Abstract. Muon hodoscope URAGAN consists of four independent supermodules with total area 46 m^2 and is under operation in the Experimental complex NEVOD (MEPhI, Moscow) from 2007. At present, the sequence of real-time data of angular variations of muon flux measured in the hodoscopic mode and also the results of their analysis: local angular anisotropy, wavelet frequencies, etc. are available at the URAGAN web-site. Some peculiarities of application of these data for the analysis of various events in heliosphere, magnetosphere and atmosphere are discussed.

1. Introduction

Muon hodoscope URAGAN [1] is located inside the campus of National Research Nuclear University MEPhI (Moscow Engineering Physics Institute), Russia (55.7º N, 37.7º E, 173 m a.s.l.) and represents a wide-aperture large area tracking detector capable of real-time reconstruction of track of each muon arriving from any directions of the upper celestial hemisphere. URAGAN detection system consists of four independent supermodules (SM) with area 11.5 m^2 each. Supermodules detect the angular distribution of the muon flux in a wide range of zenith angles (0-80º) with a high angular resolution (~1º) and with threshold energy of 0.2 to 0.4 GeV. Each supermodule represents an eight-layer assembly of streamer tube chambers with external two-coordinate *X*-*Y*-strips read-out system. Trigger condition of event detection is the coincidence of signals from the strips of 4 or more detection *X*-planes within the time gate of 250 ns. The main objective of the URAGAN is the study of the variations of the angular distribution of the muon flux caused by different atmospheric and extra-atmospheric processes [2-5]. Three SM (SM1, SM3 and SM4) are continuously under operation, but one (SM2) is used mainly for other methodical and calibration purposes. The exposition of every experimental run is divided into equal one-minute intervals within which monitoring of detection channels (~2 s) and the actual detection (~ 58 s) are carried out. Total operational "live" time is the sum of actual detection time fractions of all one-minute intervals of the exposition except of the sum of dead-times of triggered event data read-out (in total, for one-minute interval it is about 4-5 s and is varied with trigger rate). The fraction of reconstructed events with muon tracks is ~ 91% of the total intensity of 1700-1900 triggers per second. Synchronization of all SMs operation is provided by GLONASS /GPS.

2. Real-time data processing

The experimental data represent sequences of matrices (two-dimensional histograms of 90×90 cells) of the muon angular distributions accumulated during one-minute intervals. There are three matrix types with different angular cells: zenith (θ) and azimuth (φ) angles M (θ, φ), projection angles $M(\theta_X; \theta_Y)$, and also their tangents - $M(\mathrm{tg}\theta_Y, \mathrm{tg}\theta_X)$. Each matrix represents the "muon snapshot" (muonography) of the upper hemisphere limited by the detector aperture with one-minute exposure. The use of three types of matrices is due to the fact that for the subsequent analysis the information about the angular distribution in various forms may be required. Further real-time data processing includes formation of time series of averaged over one minute and 60 minutes atmospheric pressure, counting rates of reconstructed tracks (without the barometric and temperature correction) and "live" time. These series are stored in 1-minute and 60-minute daily files in a text format. Evaluation of the degree of temporary changes in the angular distribution of the muon flux is performed by comparing the value of the current flux with some average value obtained for the preceding 24 hours. Therefore on the basis of data obtained for preceding 24 hours the following values are obtained:

- matrix $M_N(\mathrm{tg}\theta_Y, \mathrm{tg}\theta_X)$: sum of averaged over 24 hours one-minute matrices, cells contain the sum over SM of the average number of events;
- live time t_{live_N}: sum over SM of the averaged over 24 hours of "live" times of one-minute frames;
- averaged over 24 hours atmospheric pressure P_N.

These values are used for estimation of changes of counting rates in every cell of the current matrix. Every 5 minutes, and at the beginning of each hour an additional processing is carried out. These results are presented on four pages of the web-site of the NEVOD complex:

- 5- and 60-minute variations of the counting rate – http://nevod.mephi.ru/uragan_data.htm;
- angular muon flux anisotropy parameters, 2D Fourier analysis, muonographies (5-minute time series) – http://nevod.mephi.ru/English/atmosphere.php;
- angular muon flux anisotropy parameters, GSE- muonographies (60-minute time series) – http://nevod.mephi.ru/English/heliosphere.php;
- wavelet-analysis – http://nevod.mephi.ru/English/wavurg.htm.

Also on the NEVOD web-site are presented:

- image files of 5- and 60-minute matrices $M(\mathrm{tg}\theta_Y, \mathrm{tg}\theta_X)$ of variations in the angular distributions in the East-North (local geographic) and GSE (Geocentric Solar Ecliptic) coordinate systems;
- image files of obtained time-series graphs.

Formation of 5- and 60-minute time series is determined by the convenience of further physical analysis of atmospheric or heliospheric (magnetospheric) processes.

3. Barometric and temperature corrections

Cosmic ray variations of the extra-atmospheric origin are of the same order as atmospheric ones. Therefore, to study the extra-terrestrial effects it is necessary to introduce corrections related with changes of the atmosphere [6]:

$$M^{cor}(\theta, \varphi, t, \Delta t) = M(\theta, \varphi, t, \Delta t) + \Delta M_P(\theta, t, \Delta t) + \Delta M_T(\theta, t, \Delta t), \quad (1)$$

here: ΔM_T and ΔM_P are corrections on temperature and barometric effects for matrix M cells. Barometric correction (barometric coefficients - B) is determined for long periods of time operation of the hodoscope, during which the atmospheric pressure varied widely. Barometric coefficients B are

determined for each cell of the angular distribution matrix, for example, $B(\mathrm{tg}\theta_Y, \mathrm{tg}\theta_X)$. The matrix of cell correction ΔM_P is calculated by the formula:

$$\Delta M_P(tg\theta_Y, tg\theta_X) = B(tg\theta_Y, tg\theta_X) \times (P_0 - P) \times t_{live}, \quad (2)$$

where t_{live} is a "live" time of the data frame.

Unlike the barometric coefficient, for temperature correction it is necessary to know the temperature profile of the atmosphere above the setup location [6]:

$$\Delta M_T(\theta) = M_0(\theta) \cdot \sum_i W_T(h_i, \theta) \Delta T(h_i) \Delta h_i / 100\%. \quad (3)$$

Here M_0 a is the averaged during long period matrix M; $W_T(h,\theta)$ are differential in altitude temperature coefficients (DTC), calculated in [7], h is the depth of the atmosphere, Δh = 0.05 atm, $\Delta T(h) = T_{SMA}(h) - T(h)$ are changes in altitude profile of the temperature, $T(h)$ is the temperature at a depth h, $T_{SMA}(h)$ is the temperature of a standard model of the atmosphere [8] at the altitude h.

Barometric correction of values of matrices is done separately for each SM using barometric coefficients for every cell of the matrix:

$$M_{ci} = M_i + B_i \cdot (P_0 - P) \cdot t_{live}^i. \quad (4)$$

Here: i is the number of the SM, M_{ci} is the corrected value in the cells of the matrix [s^{-1}]; B_i is the matrix of barometric coefficients for the cells of the current matrix [$mbar^{-1}$ s^{-1}]; P is the atmospheric pressure [mbar]; t_{live}^i is "live" time.

In the cells of the matrix, values of changes of counting rates in terms of statistical errors δ_σ are calculated as follows:

$$\delta_\sigma = \frac{M - M_N \cdot t_{live} / t_{live}^N}{\sqrt{M_N \cdot t_{live} / t_{live}^N}}. \quad (5)$$

Here matrix M_N is the sum of averaged over 24 hours one-minute matrices, cells contain the sum over SM of the average number of events; t_{live}^N is the "live" time: sum over SM of the averaged over 24 hours of "live" times of one-minute frames;

Temperature correction is introduced into the one-minute, 5-minute and hourly data. These procedures is carried out in off-line mode and are presented on the web-site with a delay, which is required to obtain data on the temperature profile of the atmosphere and to calculate the differential in altitude temperature coefficients. In particular, the information from Central Aerological Observatory (Russia, Dolgoprudny) is used (http://www.aerology.org/]. It based on the temperature profile measured by meteorological balloons two times a day: 00:00 and 12:00 UT. The data is then interpolated and the temperature correction is calculated individually for each time interval of time series data sequence. Additional data about the temperature profile of the atmosphere above the Moscow region is obtained from satellite data (http://nevod.mephi.ru/english/alice.htm).

4. Counting rate variations

On the webpage http://nevod.mephi.ru/uragan_data.htm in the section "Integral intensity mode" the graphs of 5-minute (during the last 24 hours) and 60-minute (over the last 30 days) variations averaged for three supermodules counting rates (figure 1) in terms of deviations (in percent) from the average counting rate are presented.

Counting rate variations with pressure correction are given relative to the following average values of counting rates: 1450 s^{-1}, 1412 s^{-1} and 1414 s^{-1} for SM1, SM3 and SM4 respectively.

The average counting rate of three detectors is formed in a following way:

$$I = \frac{I_1 \cdot t_{live}^1 + I_3 \cdot t_{live}^3 + I_4 \cdot t_{live}^4}{t_{live}^1 + t_{live}^3 + t_{live}^4}, \quad (6)$$

here, I_1, I_3, I_4 are counting rates of SM1, SM3 and SM4 with barometric corrections, t^1_{live}, t^3_{live} and t^4_{live} are "live" times of SM1, SM3 and SM4. Barometric coefficients of counting rates for supermodules SM1, SM3 and SM4 are -2.79 mbar^{-1}s^{-1}, -2.55 mbar^{-1}s^{-1} and -2.58 mbar^{-1}s^{-1}, respectively. Statistical error of 5-minute values of deviations of the average counting rate for all supermodules is ~ 0.1%, and for 60-minute values ~0.03% for average counting rate of three SM, and ~0.05% for supermodules separately.

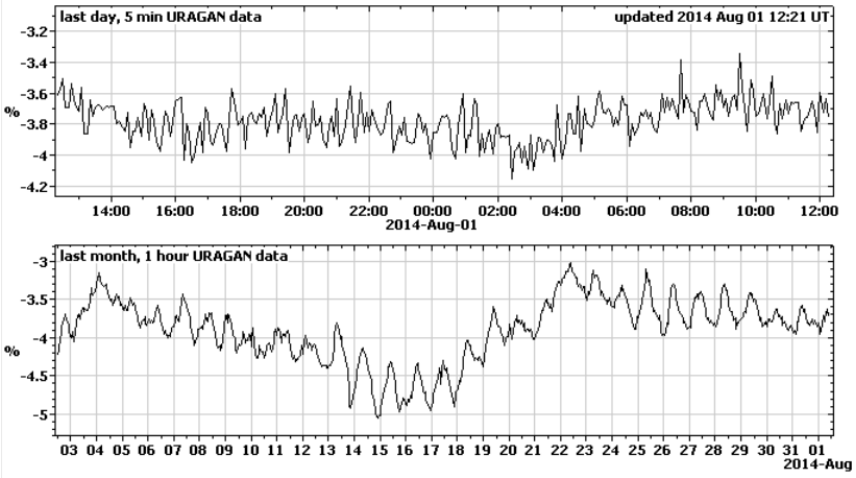

Figure 5. Averaged counting rate variations of URAGAN supermodules, normalized and corrected for atmospheric pressure.

5. Angular muon flux anisotropy

On the webpage http://nevod.mephi.ru/English/atmosphere.php the time series of characteristics of the angular distributions of 5-minute matrices $M(\theta, \varphi)$ and the results of Fourier analysis of the matrices of 5-minute changes in the counting rate δ_σ and 48 their smoothed images (within the last 2 hours) are presented.

For the analysis of the changes in the angular distribution of the muon flux according to the data of three SM the vector of local anisotropy $\vec{A}$ is used [9]. Vector $\vec{A}$ is the sum of the unit vectors of particle tracks, normalized to the number of tracks. The range of zenith angles $\theta = 0 \div 75^\circ$ and of azimuth angles $\varphi = 0 \div 360^\circ$ is used.

Horizontal projections of the local anisotropy vector on the North-South axis A_S and East-West A_E do not depend on the barometric and temperature corrections. At calculating the vertical projection A_Z the barometric correction depending on the zenith angle is used. The additional information provides a difference between the current anisotropy vector $\vec{A}$ and its average value calculated over data collected during some preceding period (in the real-time regime, $\vec{A}_N$ ($A_{N\_S} \approx 0.0031$, $A_{N\_E} \approx 0.0020$, $A_{N\_Z} \approx 0.83$) resulting from the time interval from February to November 2007 is used). The difference between these vectors $\vec{r}$ (relative anisotropy vector) and its horizontal projection r_h:

$$\vec{r} = \vec{A} - \vec{A}_N \,, \qquad r_h = \sqrt{r_S^2 + r_E^2} \tag{7}$$

indicate the direction and level of deformation of the shape of angular distribution of the particle flux.

6. Muonography

Muonography is the graphical representation of the matrices of angular distribution of the counting rate changes obtained for 5-minutes or 1-hour "live" time periods with respect to the normalized matrix during preceding 24 hours, in terms of statistical errors [10]. According to the data of three SM,

the following muonographies are formed: unsmoothed, smoothed by Gaussian low-frequency filter, with the correction of the bell-like shape of the angular distribution, in the coordinate systems East-North and GSE (Geocentric Solar Ecliptic System). If to carry out an approximation of the current and the normalized angular distributions using the dependence in the form $C \cdot cos^{\alpha}\theta \cdot d\Omega$ and obtain for them coefficients (C, α) and (C_N, α_N), respectively, it is possible to harmonize the shape of the normalized distribution in accordance with the shape of the current angular muon flux distribution reflected in the matrix. Conversion coefficient of the form of angular distribution $k(\theta)$ is:

$$k(\theta) = \frac{C \cdot \cos^{\alpha}\theta}{C_N \cdot \cos^{\alpha_N}\theta}. \quad (8)$$

Correction to the bell-shape is done to improve the image detail at possible relatively large changes of the current and normalized matrices.

On the web-page http://nevod.mephi.ru/English/atmosphere.php, a sequence of 24 pairs of images (within the last 2 hours) of 5-minute matrices of angular muon flux changes δ_σ, smoothed with the Gaussian filter (uncorrected and corrected for the shape of the angular distribution) in the East-North coordinate system are shown. Figure 2 shows one of the pairs of images of 5-minute matrices without correction for the shape of the angular distribution and with correction. The projection of matrix M to the map of the Moscow region is done in the following way. Each cell of the matrix M is projected onto the plane located at an altitude of 15 km (muon generation level) above the Earth's surface. Then the coordinates of found cells are projected on a map. Color indicates the deviation in the counting rate in terms of statistical errors.

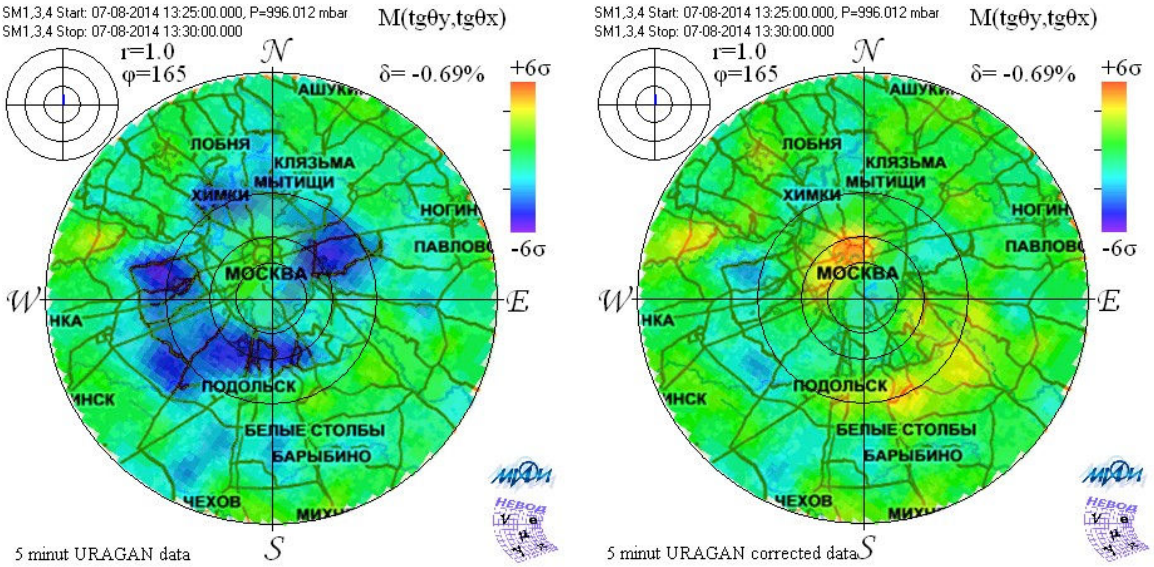

Figure 2. Example of a smoothed 5-minute matrix changes of the angular distribution of the detected particle flux in terms of statistical errors. Left - without correction for the shape of the angular distribution, right - with correction.

The figure also displays: δ which is a change in the counting rate in %, r is value of r_h and φ is the azimuth direction (in degrees) of the vector $\vec{r}$ calculated from the data of 5-minute matrix (0º is direction to the South, 90º is direction to the East). Top left, inside of small circles with radii 1, 2 and 3 (in units of $\sigma_{stat}(r_h) \approx 3.6 \cdot 10^{-4}$), the length and direction of the horizontal projection of the vector $\vec{r}$ are displayed.

On the webpage http://nevod.mephi.ru/English/heliosphere.php, the time series of the angular distribution characteristics for 60-minute matrices M are presented. Also 24 pairs of images (for the last 24 hours) of smoothed 60-minute matrices of counting rate changes δ_σ transformed from the local

coordinate system to the GSE coordinate system are presented. For the qualitative representation of the anisotropy of angular distribution of the muon counting rate changes δ_σ caused by the heliosphere disturbances, we made the transformation of the images of matrices from the laboratory system *M* observed at the detector level to the magnetopause in GSE coordinate system. GSE-mapping of detected muons is formed with the use of the pre-calculated for the location of URAGAN setup asymptotic directions of primary protons [11]. For each angular cell of the original matrix it is possible to introduce four coordinates of the cell corners $(\theta, \varphi)_{lab}$. Taking in to account the table of asymptotic direction for the corners $(\theta, \varphi)_{lab}$ we determined coordinates of the corners $(\theta, \varphi)_{GSE}$ in GSE coordinate system of transformed cell at the level of the magnetopause boundary. Thus, the variations of the muon flux of each cell of the original matrix are reflected from the laboratory system of the detector in the GSE system in the range limited by coordinates $(\theta, \varphi)_{GSE}$.

One of the pairs of GSE images of 60-minute matrices without correcting for the shape of angular distribution and with correction is shown in figure 3. The figure also represents the change in the counting rate in % (δ), the direction of the line of force of the interplanetary magnetic field (indicated by a circle with a diagonal cross), the direction to the Sun (the image of the solar corona) and asymptotic direction for vertical muons (cross).

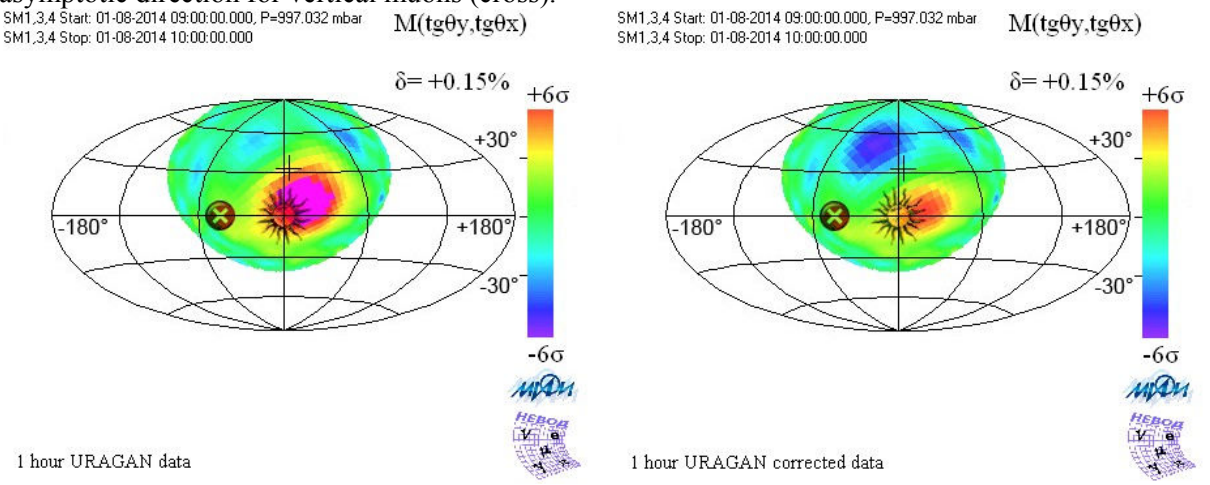

Figure 3. Example of GSE-maps of a smoothed 60-minute matrix of changes of angular distribution of the detected particle flux in terms of statistical errors. Left: without correction for the shape of the angular distribution, right: with correction.

7. 2D Fourier analysis

2D Fourier transformation of the smoothed matrix of changes without correction for the shape of the angular distribution is used to obtain a spatial-wave characteristics: P_{int} is the sum of the amplitudes of the spatial waves; P_{max} is the maximum wave amplitude among the waves with frequency greater than 1 (in relative units); *alpha* is the direction of the wave front with amplitude P_{max} (in degrees from the direction to South toward the direction to the East); *Freq* is the relative frequency of the wave with an amplitude of P_{max}.

8. Wavelet-analysis

For analysis of the different waves presenting in the data of time series of counting rate and characteristics of zenith-angular distributions, the Morlet wavelet processing is performed. Wavelet analysis is carried out immediately after the receipt of the next 5- and 60-minute time series values. At the wavelet coefficients calculating for the current time only the current and preceding time series data are used. Results of wavelet processing are presented as time dependences of amplitudes and power wavelet coefficients for periods ranging from 20 minutes to 32 hours. We use different ranges of periods for more detailed revealing of waves related with different modulation processes in the atmosphere and extra-terrestrial space.

Examples of graphic representation of time series of wavelet coefficients for total hodoscope counting rate I_{sum} for period range from 20 minutes up to 120 minutes presented on the webpage http://nevod.mephi.ru/English/wavurg.htm are shown in figures 4-5.

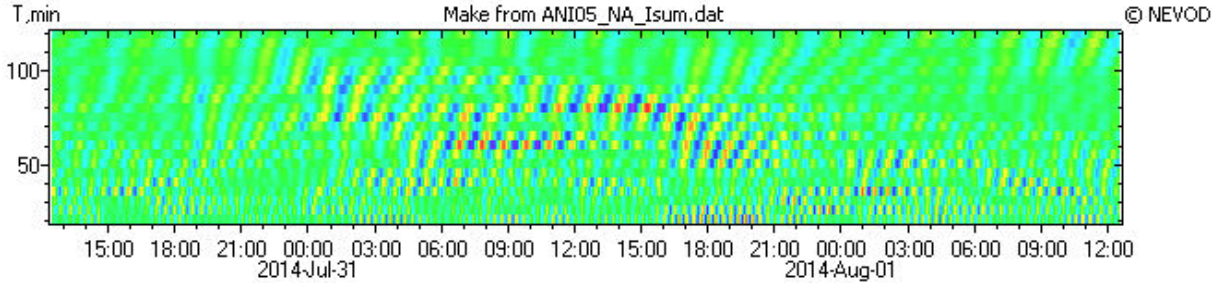

Figure 4. The real part of the wavelet coefficients for frequencies with periods from 20 minutes to 2 hours for 5-minute time series of the total counting rate I_{sum}.

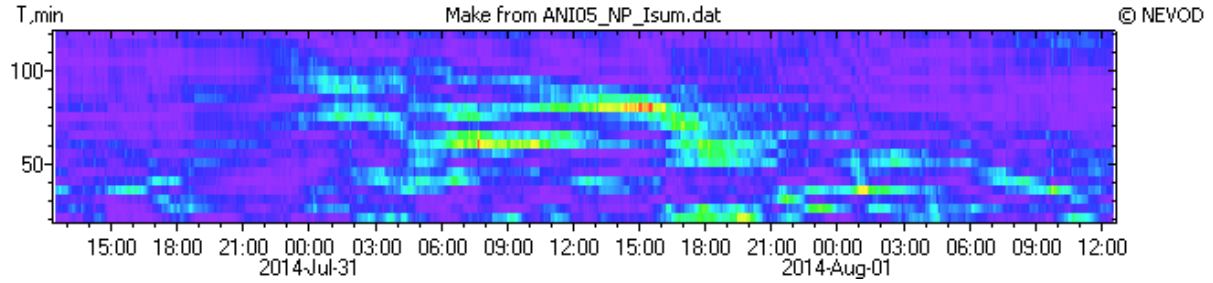

Figure 5. Power of wavelet coefficients for the frequencies with periods from 20 minutes to 2 hours in 5-minute time series of the total counting rate I_{sum}.

Color gradation (from blue to red) reflects the change in the coefficient values (from minimum to maximum) in the displayed time interval for frequencies with periods T.

9. Conclusions

Real-time data of the muon hodoscope URAGAN presented in the NEVOD web-site give possibility to analyze temporal changes not only of the counting rate of the particles but also of the characteristics of their angular distributions.

Variations of characteristics of the muon flux represented by 5-minute data are mainly due to the changes of atmospheric conditions, but they can also be caused by solar proton events, for example, GLE (Ground Level Enhancement). In contrast, variations that present in 60-minute data allow to observe mainly solar events that affect the distribution of galactic cosmic rays in the heliosphere and the Earth's magnetosphere.

The examples of analysis different kinds of atmospheric and extra-terrestrial phenomena by means of URAGAN data can be found in [12].

Acknowledgments

This work was performed at the NEVOD Scientific and Educational Center with the financial support from the State provided by Russian Ministry of Education and Science (government task and project No. RFMEFI59114X0002) and the grant of the Leading Scientific School NSh-4930.2014.2.

10. References

[1] Barbashina N S et al 2008 *Instrum. Experim. Techn.* **51** 701.
[2] Timashkov D A et al 2007 *Proc. 30th Int. Cosmic Ray Conf.* (*Merida, Mexico*) vol 1 (Mexico: Universidad Nacional Autonoma de Mexico) p 209.
[3] Timashkov D A et al 2008 *Astropart. Phys.* **30** 117.

[4] Barbashina N S et al 2009 *Bull. Russ. Acad. Sci. Phys.* **73** 343.
[5] Mikhaylenko A S et al 2011 *Bull. Russ. Acad. Sci. Phys.* **75** 827.
[6] Dorman L I 1972 *Meteorological Effects in Cosmic Rays* (in Russian, Moscow: Nauka) .
[7] Dmitrieva A N, Kokoulin R P, Petrukhin A A, Timashkov D A 2011 *Astropart. Phys.* **34** 401–411.
[8] Glagolev Yu A 1970 *Reference Book on Physical Parameters of the Atmosphere* (in Russian, Leningrad: Gidrometizdat).
[9] Shutenko V V et al 2013 *Geomagn. Aeronomy*. **53** 571.
[10] Shutenko V V et al 2013 *J. Phys.: Conf. Ser.* **409** 012193.
[11] Shutenko V V et al 2009 *Bull. Russ. Acad. Sci. Phys.* **73** 347.
[12] I.I. Yashin et al 2013 *J. Phys.: Conf. Ser.* **409** 012192